International Journal of
INTELLIGENT SYSTEMS AND APPLICATIONS IN ENGINEERING
ISSN:2147-6799 www.ijisae.org Original Research Paper

Multi-Objective Evolutionary Artificial Potential Field for Indoor Path Planning

[1]Ahmed A. Abdelaal, [2]Nesreen I. Ziedan, [3]Tamer S. Gaafar

Submitted: 04/12/2023 **Revised**: 13/01/2024 **Accepted**: 24/01/2024

Abstract: Path planning is crucial for robotics, enabling robots to find collision-free routes from their current positions to target positions. The Artificial Potential Field (APF) approach utilizes attractive and repulsive fields to guide robots towards targets while avoiding obstacles. However, the conventional APF's repulsive potential equation can yield suboptimal results due to local minima. To address this, a novel method called Multi-Objective Evolutionary Artificial Potential Field (MOE-APF) is introduced. MOE-APF modifies the repulsive potential equation and employs the membrane computing and Genetic Algorithm (GA) to optimize a new set of APF parameters. The fitness function considers multiple objectives: path length, smoothness, success rate, and safety. A comparison with a recent method called Membrane Evolutionary Artificial Potential Field (memEAPF) shows that MOE-APF significantly enhances path quality, optimization time, and success rate across various environments. MOE-APF's versatility allows it to tackle path planning challenges involving non-holonomic robots, multiple robots, industrial manipulators, and dynamic obstacles.

Keywords*: Genetic Algorithms, Optimization, Artificial Potential Field; Path Planning; Mobile Robots.*

1. Introduction

Path planning for mobile robots in indoor environments is a crucial aspect of autonomous navigation. With the rapid advancements in robotics and artificial intelligence, mobile robots are increasingly being deployed in various indoor settings such as warehouses, hospitals, and manufacturing facilities [1]. The goal of path planning is to enable these robots to efficiently and safely navigate through complex and dynamic environments, avoiding obstacles and optimizing their trajectories [2].

Path planning approaches can be classified into classical, heuristic [3, 4], and Learning-based approaches [5, 6]. Learning-based approaches use machine learning to learn path planning from data [7], by imitation [8], or using Reinforcement Learning models [9]. Hybrid classic and heuristic path planning [10] combines the strengths of both classic and heuristic algorithms to optimize path-finding in complex scenarios. Classic algorithms [11], such as Dijkstra's algorithm or A* search[12], provide a systematic and thorough exploration of the search space, guaranteeing an optimal solution. However, they can be computationally expensive and struggle with large-scale environments. On the other hand, heuristic algorithms [13], like Genetic Algorithms (GA) or Simulated Annealing, introduce randomness and heuristics to efficiently explore the search space and quickly converge towards near-optimal solutions. By integrating these two approaches, hybrid approaches [14] can leverage the efficiency and convergence speed of heuristics while ensuring the optimality provided by classic algorithms. Hybrid approaches strikes a balance between computational efficiency and solution quality, making it suitable for real-time path planning applications in dynamic and complex environments.

Amongst classic approaches, Artificial Potential field (APF) has recently gained more popularity due to its elegant mathematical model. However, it has some inherent limitations that affect its performance [15]. A review of previous studies addressed these limitations either by modifying the field equations or by integrating another algorithm is introduced in [16]. This paper introduces a novel method called Multi-Objective Evolutionary Artificial Potential Field (MOE-APF), where a multi-objective meta-heuristic algorithm is employed for automatic tuning of the modified APF parameters.

The remainder of this paper is organized as follows. In section 2, the conventional APF approach is described. In section 3, the memEAPF method is explained and its

[1]*Computer and Systems Engineering Department, Faculty of Engineering, Zagazig University, Zagazig, 44511, Egypt*
ahmed.abdelbasit.1994@gmail.com
[2]*Computer and Systems Engineering Department, Faculty of Engineering, Zagazig University, Zagazig, 44511, Egypt*
ziedan@outlook.com
[3]*Computer and Systems Engineering Department, Faculty of Engineering, Zagazig University, Zagazig, 44511, Egypt*
tamer_samy_gaafar@yahoo.com
Corresponding author: *Ahmed A. Abdelaal, ahmed.abdelbasit.1994@gmail.com*

limitations are discussed. The proposed MOE-APF method is described in section 4. Section 5 contains an investigation for hyper-parameter selection of the proposed MOE-APF method. The simulation results and the analysis are discussed and an overview of path quality in different test environments is provided in section 6. The paper is concluded in section 7.

2. Related Work

APF was first introduced in by Khatib [17] based on artificial forces exerted by attractive field of target position and repulsive fields of obstacles. The total resultant force controls the MR towards its target position while repelling it away from obstacles. The total potential field and the force applied to the MR are calculated, respectively, by:

$$U_{total}(q) = U_{att}(q) + U_{rep}(q),, \quad (1)$$

$$F(q) = -\nabla U_{total}, \quad (2)$$

where $U_{total}(q)$ is the total potential field applied on the MR at position $q = [x, y]$, U_{att} is the target attractive field, and U_{rep} is the total repulsive field exerted by obstacles, and $F(q)$ is the total resultant force exerted on the MR.

Both attractive and repulsive field equations contain proportional constants (k_a and k_r) that affect the generated path. The traditional practice of depending on the user to change these gains by try and error is a limitation of the classic APF method [14]. Moreover, the probability that the MR may fall in a local minimum position due to the equilibrium of fields is a common problem inherent in the APF method. The limitations of the classical APF approach were discussed in [15], which were categorized into four main problems; trap situations due to local minima (cyclic behavior), no passage between closely spaced obstacles, oscillations in the presence of obstacles, and oscillations in narrow passages.

Several modifications were made to enhance the effectiveness of the APF path planning method. In one category, the repulsive potential field equation was modified by adding the relative distance between the MR and the target position into the repulsive field equation so that there is a single global minimum at the target position [18]. The modified force exerted by an obstacle on the MR at position q can be calculated by:

$$F_O(q) = k_r \left(\frac{1}{\rho} - \frac{1}{\rho_0}\right) \times \frac{1}{\rho^2} \times (q_t - q), \quad (3)$$

where the subscript o denotes the obstacle, k_r is the repulsive proportional constant, ρ is the shortest distance between the MR and obstacle, ρ_0 is the distance of influence for the obstacle, and q_t is the target position.

In a second category, meta-heuristic algorithms including GA [19], Particle Swarm Optimization (PSO) [20, 21], Ant Colony Optimization (ACO) [22], and Membrane Evolutionary Algorithm [23] were employed to optimize the APF parameters. Specifically, these algorithms were used to fine-tune the attractive proportional (k_a), repulsive proportional (k_r), and step size (η) parameters, resulting in improved path planning performance. In a third category, a rotational component was introduced to the repulsive field, guiding the mobile robot along the contour of obstacles rather than simply repelling it away [24-26]. In addition, the Wall-Following (WF) method was used to enable the MR to escape from local minima positions by following the obstacle contour or simply by adding a virtual force component that repel the MR away from this position [18, 27]. These modifications collectively enhance the ability of the APF algorithm to navigate through complex environments and optimize path calculation.

Recently, the APF was employed with different modifications in many applications. In [28], the Dynamic Artificial Potential Field (D-APF) was employed for Unmanned Aero Vehicle (UAV) to follow Ground Moving Targets (GMT). Both attractive and repulsive functions in D-APF were modified to include the relative distance and speed between the UAV and both of the target and obstacles. In [29], the Black Hole Potential Field (BHPF) was employed with a Reinforcement Learning (RL) model to solve the local stable points in multi-target environments such as warehouses. The attractive potential field was combined with the black-hole domains so that attractive force guides the MR to the nearest target directly without being affected by other targets' fields. The RL model enhanced the adaptability of the MR to the changes of obstacles types and the dynamic targets. In [30], a modified ACO algorithm was employed with a dynamic step-size selection mechanism to improve the APF performance. An initial path was generated using a global known map. Following that, a local planner was applied to avoid unknown obstructions detected by the USV sensors along the initial path. In [31], the Virtual Potential Field Detection Circle Model (VPFDCM) was introduced. The VPFDCM was based on an adaptive selection of the detection radius of obstacles around the MR. In addition, a Long Short Term Memory (LSTM) model is employed to predict the next state of dynamic obstacles based on saved information from previous observations. A reward was evaluated

based on safety factors and was used in a Q-Learning algorithm to optimize the VPFDCM.

In [32], the Predictive Artificial Potential Field (PAPF) was introduced. The key idea behind the PAPF was the prediction of local target positions that minimize energy consumption by reducing the MR steering actions. An initial path was generated and a selection strategy was employed to predict the position of next local target. A new path was calculated to guide the MR to the local target instead of the main target. The PAPF managed to generated smooth paths with minimized steering actions. In addition, for local trap positions, a heavy particle called top quark was placed in the local minimum position to repel the MR away.

The proposed method in this study is based on the memEAPF method introduced in [23]. The novelty of the proposed method is that it includes multiple objectives in the evaluation of the calculated paths. In addition, the repulsive field is modified to include a rotational component which helps increasing the success rate of solutions generated by the GA and membrane computing. The next section describes the previous memEAPF method and the key strength and weakness points.

3. Previous MEMEAPF

In [23], an enhanced APF algorithm called Membrane Evolutionary Artificial Potential Field (memEAPF) is introduced. The memEAPF combined membrane computing with the GA to optimize the APF parameters which were k_a, k_r, and η. The attractive field of the target position is calculated by:

$$U_{att}(q) = \frac{1}{2} k_a (q_t - q)^2. \quad (4)$$

The total the repulsive field exerted by the obstacles is calculated by:

$$\boldsymbol{U_{rep}(q) = \sum_o U_o(q),} \quad \textbf{(5)}$$

$$\textbf{where } \boldsymbol{U_o(q)} = \begin{cases} \frac{1}{2}\boldsymbol{k_r}\left(\frac{1}{\rho} - \frac{1}{\rho_0}\right)^2 & \boldsymbol{\rho \le \rho_0} \\ \mathbf{0} & \boldsymbol{\rho > \rho_0} \end{cases} \quad \textbf{(6)}$$

In the memEAPF, the set of solutions, called population [33], is divided into subgroups, called membranes. Each elementary membrane contained arrays of multisets of objects, called individuals, comprising sets of parameters, which were the proportional gains and step size. The memEAPF employed a one-level membrane structure with rules such as membrane merger and division. The membrane merger played a beneficial role in enhancing information communication among individuals, while the membrane division contributed to improving the search capability. Evolution rules consisting of merge, communication, and divide stages governed the behavior of the elementary membranes.

The computational process consisted of several steps. In the first step, each elementary membrane evolved the individuals within it using an evolutionary artificial potential field (EAPF). Where the GA applied evolution cycles with path length resulting from the APF as the fitness value of every individual solution. Each individual solution was represented by a set of parameters $[k_a, k_r, \eta]$. The primary objective of this stage was to identify the best individual solution within each elementary membrane.

In the second step, all the elementary membranes merged into a single membrane, which contained all the individuals. Communication rules were applied. Initially the rules separated the best individual from each elementary membrane to identify the global best individual $[k_a, k_r, \eta]_{best}$. A copy of this global best individual was then transmitted to the skin membrane to preserve the current global best solution. The communication process continued within the merged membrane, facilitating the exchange of information among the elementary membranes that would be formed in the subsequent step. Throughout the merger process, each subpopulation was maintained. The worst individuals, constituting a portion of the subpopulation, were replaced by copies of the best individuals to enhance the subpopulation within each elementary membrane.

The memEAPF demonstrated the capability to generate feasible paths in both static and dynamic environments, undergoing testing in both sequential and parallel implementations. However, the optimization process proved to be excessively time-consuming, exceeding 300 seconds in certain test scenarios for two reasons. First, the step size was an optimization parameter, which could be selected in small values. Small step size resulted in a large number of configuration points to be calculated along the paths. Second, the conventional field equations made it easy to fall in local minima. Therefore, the memEAPF suffered from an increase in the fail rate. Accordingly, the memEAPF required a large number of generations to guarantee finding parameters that could generate a feasible path. In addition, using a fixed distance of influence in the memEAPF method increased the fail probability to pass through narrow passages. These limitations make the memEAPF not suitable for real-time applications.

The evolutionary algorithm employed a sole criterion for selecting the best solutions, which was the path length.

The absence of path smoothness as a selection criterion in the fitness function gave rise to oscillations in the resulting paths. In this paper, the shortcomings of the memEAPF are addressed by exploring a more convenient path planning method. The proposed MOE-APF method incorporates multiple objectives, which are minimizing the optimization time and path length, and improving path smoothness, path safety, and success rate in finding feasible paths that overcome the local minima positions.

4. The Proposed MOE-APF Method

The MOE-APF method is based on a modified APF repulsive field together with an evolutionary algorithm that optimizes a different set of APF parameters. To overcome the local minima and increase the success rate, the repulsive potential field is modified by adding two factors. The first factor, which was proposed in [18], is adding the relative distance between the robot and the target position to ensure that there is only one global minimum at the target position. The second factor, which was proposed in [25, 27], is adding a rotation matrix with angle θ_r so that the obstacle forces the MR to rotate around it rather than just repelling the MR away from it. The rotation angle used by Li [25] was set to zero or 60 based on a detection criteria for a local minima position. In [26], the rotation angle was set for each obstacle separately to either 90 or -90 based on the angle between the MR trajectory and the vector from the MR and the obstacle centroid.

In the proposed MOE-APF method, both factors are incorporated. The rotation angle is added to the optimization parameter that the evolutionary algorithm tries to get the best fit value. Moreover, to reduce computation time and enhance the path quality, a limited view angle of $\frac{\pi}{3}$ is set so that only obstacles lying between the robot and the target will affect the MR movement. The new repulsive force exerted by an obstacle can be calculated by:

$$\vec{F}_o(q) = \begin{cases} \begin{vmatrix} \cos(\theta_r) & -\sin(\theta_r) \\ \sin(\theta_r) & \cos(\theta_r) \end{vmatrix} \times k_r \left(\frac{1}{\rho} - \frac{1}{\rho_0}\right) \times \frac{1}{\rho^2} \times \|q_t - q\| \times \frac{\overrightarrow{q_{OR}}}{\|\overrightarrow{q_{OR}}\|} & if\ |\theta_{RO-RT}| < \frac{\pi}{3}\ and\ \rho \le \rho_0 \\ 0 & otherwise, \end{cases} \quad (7)$$

where $\theta_{\mathrm{RO-RT}}$ is the angle between the vector from the MR to the target and the vector from the MR to the obstacle, and $\overrightarrow{q_{OR}}$ is the vector from the obstacle position to the MR position.

Solving the local minima problem increases the success rate for the APF algorithm, which in turn reduces the number of generations required to converge to a feasible path. Moreover, the need for adapting the step size to each environment does not exist anymore. Instead, a fixed value can be used based on a statistical investigation. The selection of step size is discussed in the next section.

The membrane computing and GA are used to optimize a different set of APF parameters, which are the attractive field proportional k_{a}, the repulsive field proportional k_r, the distance of influence for obstacles ρ_0, and the rotational angle of repulsive field θ_r. In the MOE-APF method, the distance of influence is added to the set of optimization parameters so that the algorithm can choose a small value in narrow passage cases and the MR can move smoothly towards the target position.

The fitness function used by the evolutionary algorithm in MOE-APF is modified to consider multiple objectives, which are path length, path smoothness, success rate, and path safety. The modified fitness function can be calculated by:

$$fitness = l + r + C_f + C_c \quad (8)$$

, where l is the path length, r is the path roughness, C_f is the fail penalty, and C_c is the collision penalty.

The fail penalty and the collision penalty are large constants equal to 200 and 400 respectively. The fail penalty is added to the fitness value in case the resulting path cannot reach the target position. Similarly, the collision penalty is added to the fitness value in case the resulting path intersects any of the obstacles. Both penalty constants are added to the fitness value to mark the set of APF parameters $[k_a, k_r, \rho_0, \theta_{\mathrm{r}}]$ that would result in bad solutions and so it will be eliminated in the selection stage of the evolutionary algorithm. The multi-objective path planning was introduced in [34] and included path length, path smoothness, and path safety. Path smoothness was calculated in terms of the absolute difference in orientation between two successive configuration points along the path. Meanwhile the path safety was calculated in terms of the minimum distance between the MR and closest obstacle along the path. In the proposed MOE-APF, the path safety is added as a constant number to reduce the computation complexity, and the path length and path roughness are calculated by:

$$l = \sum_{i=1}^{N-1} |q_{i+1} - q_i|, \quad (9)$$

$$r = \sum_{i=1}^{N-1} (\theta_{i+1} - \theta_i)^2, \quad (10)$$

where θ_i is the MR heading angle with regard to the environment frame at configuration point number i, and N is the total number of configuration points in the resulting path.

The change in heading angle is squared in roughness calculation because the absolute value is not a good indicator for path smoothness as can be shown in Fig 1.The three paths shown in Fig 1 have the same value of

total absolute change of orientation. However, it is obvious that path (a) is the best trajectory for the MR, path(b) is intermediate, while path (c) is the worst. This is because the sudden change in orientation means that the MR should stop and applies a steering command. It then continues the path and this will take more travel time. The settings of the MOE-APF and the memEAPF are shown in **Table 1**.

(a) (b) (c)

Fig 1. Shows three paths with equal total absolute change of orientation equals to $\frac{\pi}{2}$, while summation of squared change is 0.352 for path (a), 0.822 for path (b), and 2.47 for path (c).

Table 1: Settings of the memEAPF and the proposed MOE-APF method

Parameter	The memEAPF method	The proposed MOE-APF method
Optimized parameters	$k_a, k_r, and\ \eta$	$k_a, k_r, \rho_0\ and\ \theta_r$
Fixed parameters	$\rho_0 = 2r_o, and\ \theta_r = \pm\frac{\pi}{2}$	$\eta = 0.4\ m$
Number of membranes	2, 4, 8, and 16	2
Total population size	16 in each membrane	64 in total
Selection rate	0.5	0.2
Mutation rate	0.2	0.15
Number of generations	100	10
Max configuration points	2000	50
Range of k_a and k_r	[0, 10]	[0, 5]
Fitness function	Path length	Path length, roughness, and safety

5. Investigating the Selection of Hyper-Parameters

5.1. *Selection of step size*

A comprehensive test is conducted to study the effect of step size on path quality in terms of path length, optimization time, path smoothness, success rate and path safety. A range from 0.05 to 1.00 meter with separation 0.05 meter is examined against the set of 12 test environments. A score function is used to evaluate the performance of each step size value. The score function includes the set of performance measures, which can be calculated by:

$$score(\eta) = \sqrt{l_\eta^2 + t_\eta^2 + r_\eta^2} + 10 \times \left(\frac{F_\eta}{F} + \frac{C_\eta}{C}\right) \quad \textbf{(11)}$$

,

where l_η, t_η, and r_η are the normalized path length, normalized optimization time, and normalized path roughness respectively evaluated for a step size η. F_η and C_η is the number of fails and collision cases for a step size η. F and C are the total number of fails and collision cases for all tested step size values.

A total of 3000 independent runs of the MOE-APF are conducted for each step size value divided equally for each test environment. For each run, the same initial population is used with all step size values so that the only varied factor is the step size itself. The average path length, average optimization time, and average path roughness are recorded in **Table 2** with the number of fails and collision cases. The minimum, maximum, and range values are calculated to get the normalized value of each performance measure in each test case. The normalized value of some performance measure (p) can be calculated by:

$$p_{normalized} = \frac{p - p_{min}}{p_{max} - p_{min}}. \quad (12)$$

To figure out how the step size affects path safety, Fig 2 shows how a large step size can lead to a higher collision probability. The red circles represent the obstacle, the small green circle represents the target position, and the rectangles represents the MR at successive time instants. The dashed line represents the limit distance of influence (ρ_0) for the repulsive field exerted by the obstacle. Fig 2 (a) shows a scenario where the resultant potential field at a position outside the distance of influence can guide the MR towards the obstacle. Therefore, making a large step in this direction will cause a collision. Meanwhile, a small step size, as shown in Fig 2 (b), allows the MR to recalculate its direction once it becomes inside the distance of influence of the obstacle before reaching the obstacle.

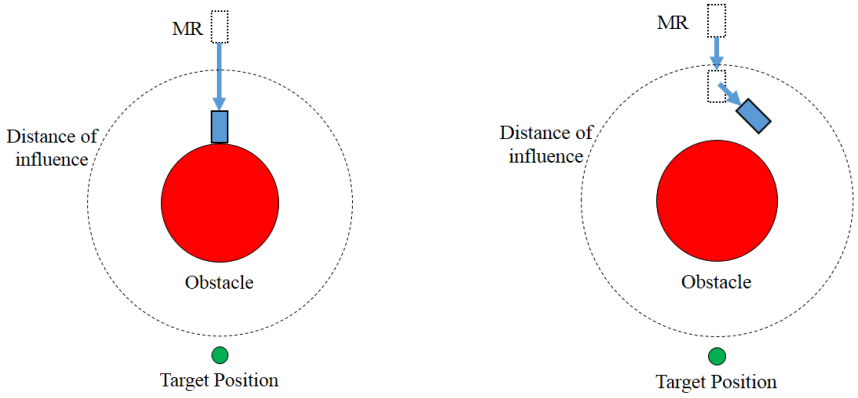

(a) large step size (b) small step size

Fig 2: shows the effect of large step size on collision probability of the MR

Table **2** shows the resultant performance measures, along with the corresponding score value calculated by (11) for each step size. As shown in the results in **Table 2**, a small step size results in shorter and smoother paths. However, there is an increase in the number of failed cases due to the local minima. In addition, the optimization time significantly increases due to the large number of configuration points in the path. On the other hand, a large step size improves the optimization time and the success rate. This is because a large step size enables the MR to cross local minima spots that may appear along the path. However, a large step size increases path roughness and path length. This is because large step size leads to a significant change in field distribution between every two successive configuration points. As a result, the MR suffers from a sudden change in orientation at every position, which, in turn, increases the path roughness. To sum up, there is a tradeoff between the performance measures that are considered in this study. The score value calculated by (11) is shown in ***Fig 3*** to give an overview about the performance of each step size.

Table 2: Performance measures of memEAPF for each tested value of step size.

	Step size	**Path length**	**Optimization time**	**Path roughness**	**Passed Cases**	**Failed Cases**	**Collision**	**Score**
	0.05	7.492	1.307	0.702	2975	24	1	4.544

	0.1	7.555	0.750	0.783	2987	12	1	2.377
	0.15	7.526	0.552	0.697	2986	12	2	2.279
	0.2	7.554	0.458	0.750	2993	4	3	1.218
	0.25	7.591	0.398	0.885	2994	5	1	1.292
	0.3	7.628	0.361	0.885	2998	1	1	0.764
	0.35	7.705	0.331	1.033	2997	3	0	1.250
BEST	0.4	7.712	0.312	0.851	2999	0	1	0.735
	0.45	7.766	0.291	0.977	2998	1	1	1.111
	0.5	7.788	0.277	0.948	2997	1	2	1.236
	0.55	7.764	0.262	0.906	2996	0	4	1.231
	0.6	7.785	0.251	0.959	2998	0	2	1.098
	0.65	7.811	0.235	0.952	2994	1	5	1.631
	0.7	7.772	0.233	1.088	2996	0	4	1.456
	0.75	7.792	0.226	1.237	2990	0	10	2.390
	0.8	7.856	0.221	1.166	2985	4	11	3.079
	0.85	7.761	0.201	0.977	2986	1	13	2.476
	0.9	7.779	0.189	1.072	2993	0	7	1.792
	0.95	7.779	0.195	1.105	2992	0	8	1.950
	1	7.901	0.205	1.230	2989	1	10	2.697
Min		7.492	0.189	0.697				
Max		7.901	1.307	1.237				
Range		0.409	1.118	0.540				

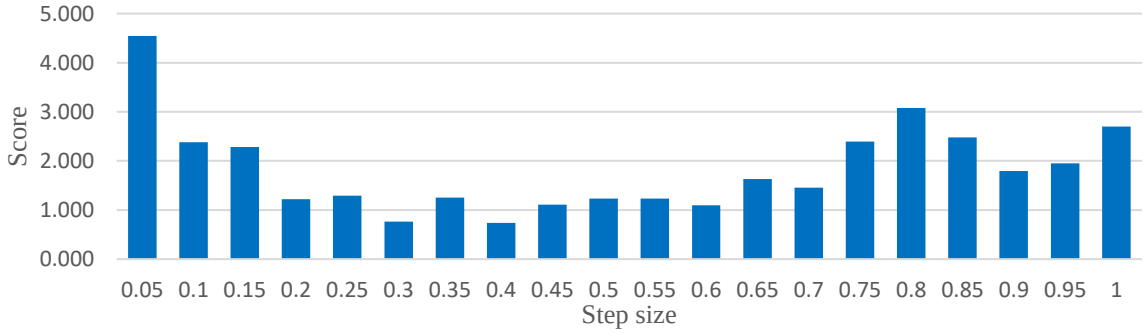

Fig 3: The relation between score value and the step size

Though the conducted investigation, it can be concluded that a step size of 0.4 meters gives the best performance in terms of path length, path smoothness, optimization time, success rate, and path safety. This value is used in all upcoming tests.

5.2. *Selection of hyper-parameters for meta-heuristic algorithms*

A comprehensive test is done to select the best hyper-parameters for the proposed MOE-APF using MATLAB. The MOE-APF algorithm is evaluated by varying the number of membranes, selection rate, and

mutation rate. The tested range for each varied hyper-parameter is recorded in **Table 3**

Table 3: The range of each varied hyper-parameter of meta-heuristic algorithms

Hyper-parameter	Minimum value	Maximum value	Step
Number of membranes	2	4	2
Selection rate	0.10	0.50	0.05
Mutation rate	0.05	0.80	0.05

A total of 69120 independent runs are conducted with 240 runs for each unique set of hyper-parameters (selection rate, mutation rate, number of membranes) distributed equally over the 12 test environments. The results indicate that setting the step size to 0.4 meters reduces the probability of fails and collisions to 0.00032 so that fail and collision cases can be considered as outlier cases and neglect their part in score equation. The new score value in this test is calculated as:

$$\boldsymbol{score(p)} = \sqrt{\boldsymbol{l_p^2 + t_p^2 + r_p^2}}\,, \qquad \textbf{(13)}$$

where p is the hyper-parameter for which the score is calculated.

The performance measures obtained using this score function is recorded in **Table 4** and **Table *5***, showcasing the results for each hyper-parameter range of values. Furthermore, **Fig 4** and **Fig *5*** are added to visualize the performance measures, allowing for a comparative analysis of the hyper-parameters performance and an easy selection of best value.

Table 4 and Fig 4 show the calculated score for each tested selection rate value. Each value of recorded path length, optimization time and path roughness is an average of 7680 runs. The results show that increasing the selection rate narrows the selection of parents, reducing diversity and leading to lower-quality solutions. Meanwhile, setting the selection rate to low percentage maintains a few good parents in next generations. A selection rate of 0.2 is proved to be optimal because it maintains a diverse population, allowing for exploration of the solution space and avoiding local optima. Therefore, there is a balance between exploration and exploitation, resulting in high-quality solutions

Table 4: Performance measures of MOE-APF for each tested value of selection rate.

	Selection rate	Path length	Optimization time	Path roughness	Passed cases	Failed cases	Collision cases	Score
	0.1	7.715	0.403	1.152	7667	2	11	0.742
	0.15	7.715	0.406	1.213	7675	1	4	1.015
Best	0.2	7.714	0.413	1.010	7678	0	2	0.362
	0.25	7.709	0.421	1.085	7680	0	0	0.739
	0.3	7.712	0.423	1.118	7678	0	2	0.892
	0.35	7.722	0.427	1.026	7679	0	1	0.877
	0.4	7.727	0.428	1.105	7679	1	0	1.093
	0.45	7.748	0.433	0.991	7678	0	2	1.414
	0.5	7.740	0.429	1.011	7679	1	0	1.201
Min		7.709	0.403	0.991				
Max		7.748	0.433	1.213				
Range		0.039	0.029	0.222				

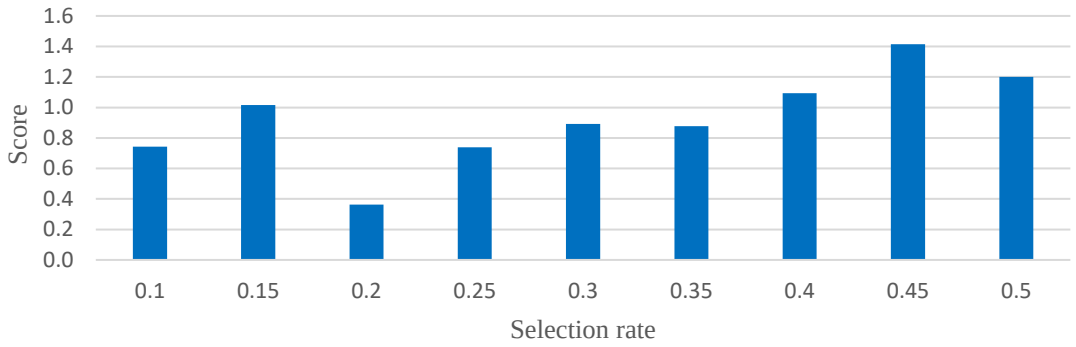

Fig 4: Bar chart of score value calculated for each tested selection rate

The mutation rate in GA is a critical parameter that affects the exploration of the search space and the diversity of the population. **Table 5** shows the recorded performance measures for each tested mutation rate together with the score value calculated by equation (13). Each value of recorded path length, optimization time and path roughness is an average of 4320 independent runs. The results indicate that increasing the mutation rate beyond 0.15 decreases the quality of the solutions. This occurs because a higher mutation rate leads to excessive exploration, causing the algorithm to lose the beneficial genetic information acquired through previous generations. Consequently, the population may struggle to converge towards optimal solutions and may exhibit reduced performance. Meanwhile, decreasing the mutation rate below 0.15 results in bad exploration and maintaining the same properties of initial parents through all generations. Therefore, the results prove that a mutation rate of 0.15 achieves a balance between exploration and exploitation. This balance allows for the introduction of new genetic material while preserving the valuable information needed for high-quality solutions in a GA. Fig 5 visualizes the calculated score for each tested mutation rate value

Table 5: Performance measures of MOE-APF for each tested value of mutation rate

	Mutation rate	**Path length**	**Optimization time**	**Path roughness**	**Passed cases**	**Failed cases**	**Collision**	**Score**
	0.05	7.746	0.376	1.340	4310	0	10	1.269
	0.1	7.696	0.383	1.102	4317	0	3	0.552
Best	0.15	7.679	0.397	1.012	4319	1	0	0.421
	0.2	7.675	0.407	0.889	4319	0	1	0.443
	0.25	7.674	0.406	1.051	4317	0	3	0.566
	0.3	7.705	0.416	1.009	4317	1	2	0.722
	0.35	7.693	0.419	1.003	4319	0	1	0.703
	0.4	7.728	0.423	0.875	4320	0	0	0.881
	0.45	7.730	0.429	1.053	4320	0	0	1.040
	0.5	7.721	0.431	1.105	4319	1	0	1.050
	0.55	7.731	0.435	1.003	4320	0	0	1.070
	0.6	7.744	0.436	1.017	4320	0	0	1.172
	0.65	7.755	0.438	1.135	4319	1	0	1.357

	0.7	7.767	0.441	1.003	4317	1	2	1.385
	0.75	7.761	0.443	1.332	4320	0	0	1.657
	0.8	7.755	0.447	1.332	4320	0	0	1.651
Min		7.674	0.376	0.875				
Max		7.767	0.447	1.340				
Range		0.093	0.071	0.465				

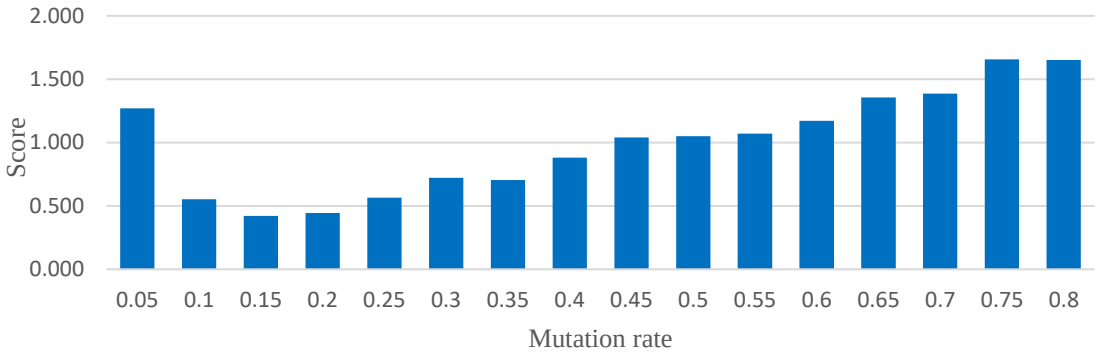

Fig 5: Bar chart of score value calculated for each tested mutation rate

The number of membranes does not show a significant effect on the generated path quality. Therefore, the number of membranes is set to 2 to reduce the execution time resulted by membranes operations. This systematic testing approach, incorporating tables and figures, ensures an effective selection of hyper-parameters and facilitates improved optimization outcomes for the proposed MOE-APF algorithm.

6. Testing and Results

The performance of proposed MOE-APF is compared with the memEAPF, where the following settings are followed:

- The memEAPF and the proposed MOE-APF are tested against a series of 12 test environments, which represent multiple challenges [15] for many MR path planning algorithms that use the APF approach.
- For each test environment, a total of 500 independent run is conducted and, in each run, the same randomly selected population size is given for both memEAPF and the proposed MOE-APF.
- The number of generations is limited to 10 for both memEAPF and MOE-APF to test the capability of each algorithm to get solution within a time limit.
- The number of membranes is set to 2, and the number of individuals in each membrane is set to 32.
- Each element in an individual solution is encoded in a 16-bit string.
- The evaluation of performance measures for the tested methods is introduced in terms of path length, path roughness, success rate, and optimization time.
- The maximum number of configuration points is set to 400 for the memEAPF so that the path length can reach 20 meters when the smallest step size value is selected. A distance of 20 meters is greater than the longest path from the start position to the target position in all environments. Meanwhile, the maximum number of configuration points is set to 50 in the proposed MOE-APF.
- In memEAPF, the spin direction of repulsive field in set manually to either clockwise or anti-clockwise direction for each test environment so that the selected value guarantees a successful generation of feasible paths.
- All the experiments are carried out on an AMD Ryzen 5 PRO 4650G CPU (3.666 GHz) with 16 GB of DDR4 RAM running Windows 11 and MATLAB 2018. Experiment data is saved in CSV format for further investigations.
- Analysis, statistics, and bar charts are generated using IBM SPSS Statistics version 28.0.0.0 (190).

In terms of success rate, Table 6 provides the number of passed and failed cases for both methods. The success

criterion comprises two conditions. First, the distance between the MR and the target position should be less than or equal to the step size length. Second, the path roughness should not exceed 5. A path with roughness greater than 5 indicates excessive oscillations, which is undesirable for MRs during path execution.

The recorded values show that the memEAPF has an average success rate of 49.42%, while the proposed MOE-APF achieves an average success rate of 98.56%, representing a significant improvement. The test environments can be categorized into three groups based on the success rate of both methods. The first group includes environments 1, 2, 5, 9, 11, and 12, where both methods exhibit a high success rate. The second group comprises environments 3, 4, 6, 7, and 10, where the MOE-APF performs well while the memEAPF struggles. The third group consists of environment number 8, which poses a challenge for both methods. To identify common features within each group, **Fig 6** displays the layout of environments in the three groups.

Environments in group 1, shown in **Fig 6** (a), share a common feature that the MR needs to apply a single maneuver along the shortest path without any obstacles directly obstructing the direct path to the target position by introducing a local minimum position. Additionally, obstacles form clusters, with only one cluster active at a time, guiding the MR along the correct path. Environments in group 2 , shown in **Fig 6** (b), present three challenges for the memEAPF. The first challenge is trap situations represented in environment 4. The second challenge is obstacles directly facing the MR and aligned with the target position forming local minima positions, which are represented in environments 3 and 6. The third challenge is narrow passages, which is represented in environments 7 and 10. In environments 7 and 10, obstacles form clusters on both sides of the MR, resulting in either local minima positions or high oscillations that affect the path quality due to a constant intersected distance of influence from obstacles on both sides. Environment 8 in group 3, shown in **Fig 6** (c), introduces a new challenge that requires the MR to maneuver with different rotation angles. Consequently, a single selection for the rotational repulsive field fails to guide the MR along the shortest path without producing high oscillations.

In terms of path length and path roughness, Figure 7 and Figure 8 present a comparison between the performance of the proposed MOE-APF and the memEAPF in terms of average path length and path roughness. The success criterion comprises two conditions. First, the distance between the MR and the target position should be less than or equal to the step size length. Second, the path roughness should not exceed 5. According to this success criteria, the memEAPF demonstrates complete failure in environments 4 and 8, as indicated by the absence of any successful runs. This highlights the limitations of the memEAPF in handling specific challenges posed by these environments. The key point of MOE-APF good performance is that a variable field of influence enables the selection of high and low values that best fits the planning challenge. On one hand, for narrow passages, selecting a small distance of influence for obstacle repulsive field generates a path free of unnecessary repulsive forces, which cases oscillations. This performance can be deduced from the calculated paths in environments 4, 5, and 10 as shown in Figure 10. On the other hand, for environment of single obstacles cluster such as environments 1, 3, and 9 as shown in Figure 10, selecting a relatively high distance of influence allow an early detection for the obstacle. Therefore, the MR can move smoothly around the obstacle rather than getting a sudden steering near the obstacle. The significant improvement in path length and path smoothness offered by the MOE-APF underscores its superior optimization capabilities and ability to find more efficient routes for the MR. This improvement holds true across all test environments, indicating the robustness and effectiveness of the proposed method

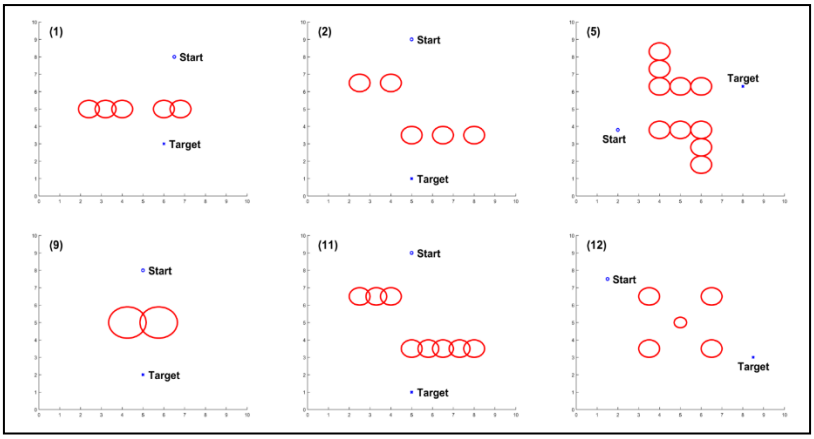

(a) Environments group 1

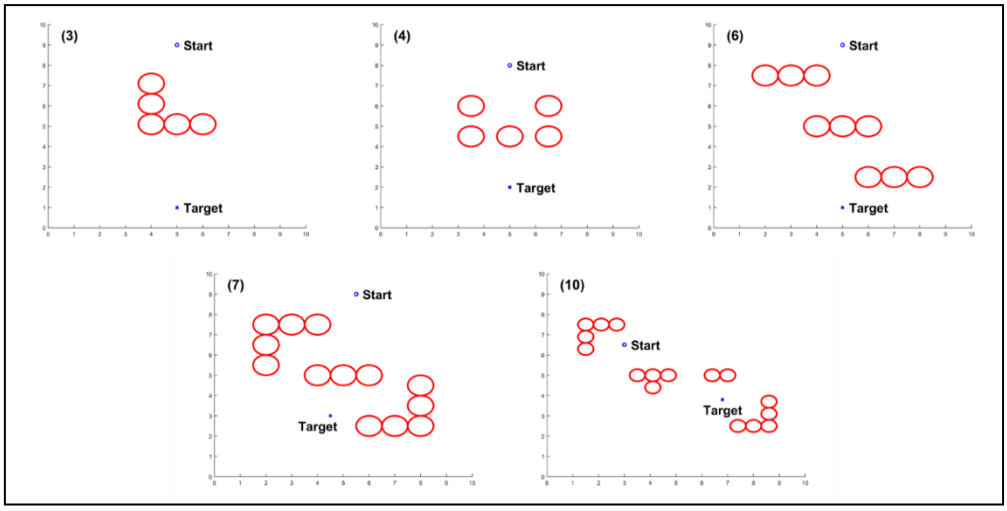

(b) Environments group 2

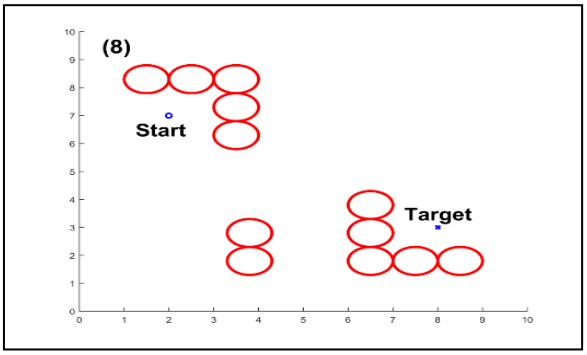

(c) Environments group 3

Fig 6: Environments categorization based on success rate of the memEAPF and the proposed MOE-APF

Table 6: Comparison between the memEAPF and the proposed MOE-APF method in terms of number of passes cases

	memEAPF		**MOE-APF**	
Environment	Passed	Failed	Passed	Failed
1	500	0	500	0
2	472	28	500	0
3	6	494	499	1

4	0	500	500	0
5	500	0	500	0
6	9	491	499	1
7	9	491	500	0
8	0	500	424	76
9	498	2	492	8
10	30	470	500	0
11	500	0	500	0
12	441	59	500	0
TOTAL	2965	3035	5914	86

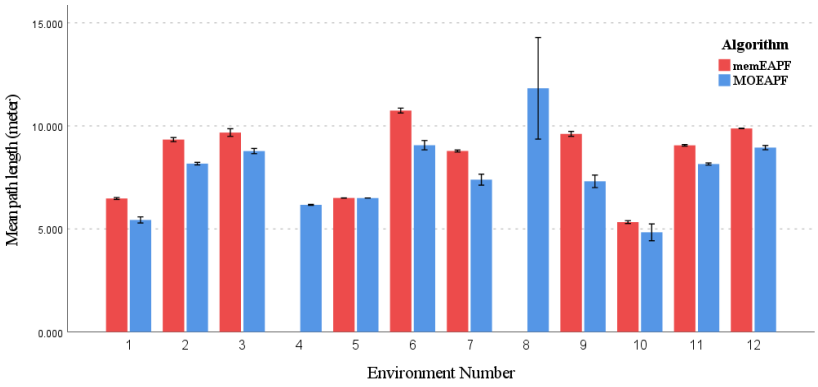

Fig 7: Comparison between the memEAPF and the MOE-APF methods in terms of path length

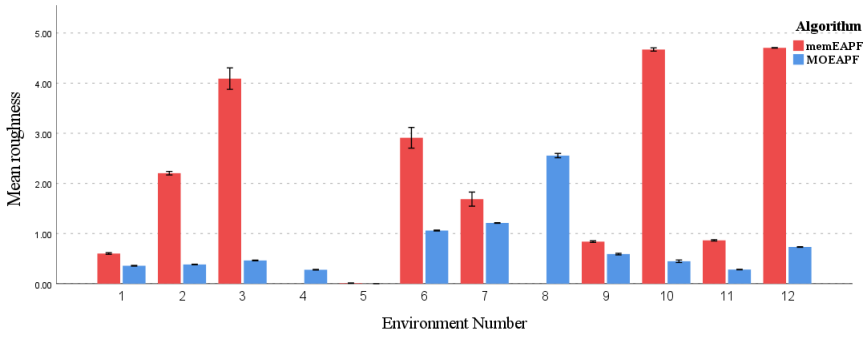

Fig 8: Comparison between the memEAPF and the MOE-APF methods in terms of path roughness

In terms of optimization time, the proposed MOE-APF proves the ability to generate feasible paths in less time for all test environments. This time reduction is mainly caused by two factors. First, setting the step size to 0.4 meters reduced the total number of configuration points that should be calculated along the path. Second, the idea of optimizing the repulsive rotational angle results in higher success rate of most individuals in the evolutionary population. Therefore, a few number of generations is required to guarantee reaching a good solution.

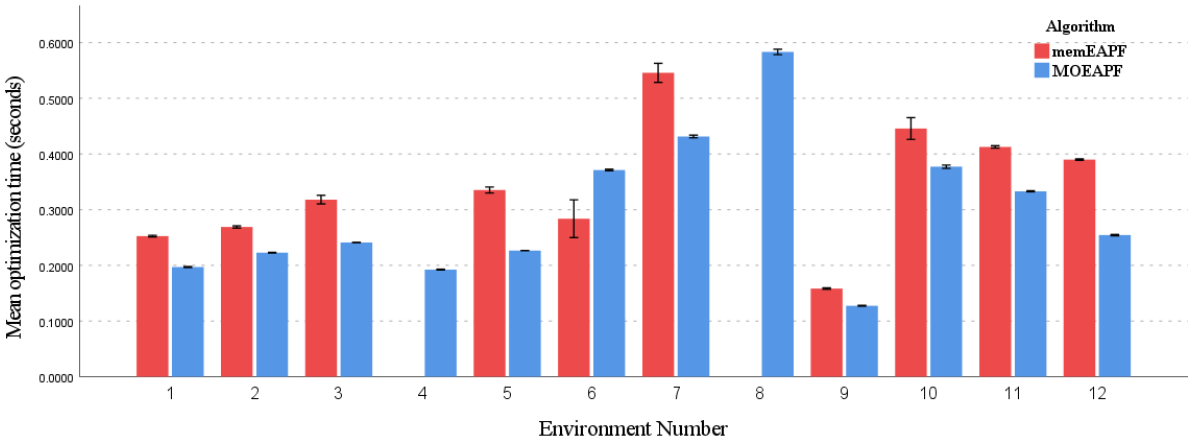

Fig 9: Comparison between the memEAPF and the proposed MOE-APF in terms of optimization time

6.1. *Demonstration of best paths calculated by the memEAPF and the MOE-APF methods*

Fig 10 presents the best results obtained from applying the memEAPF and the MOE-APF methods to the set of 12 test environments, each representing a unique path planning challenge. The path generated by the memEAPF method is represented by the dashed line, while the path generated by the proposed MOE-APF method is represented by the solid line. The start position of the MR is represented by a blue circle, and the target position is represented by a green triangle. It can be noticed that the proposed method generates shorter and smoother paths compared with the memEAPF method in all test environments. In environment 8, it can be noticed that a single field rotation angle made it difficult for the MR to maneuver both obstacles' groups placed in opposite directions of the MR. Therefore, the path was interrupted and a sudden steering is made before the second obstacles' group. An online path planning approach can be incorporated to continuously calculate the best rotational angle so that the MR can maneuver different obstacles along its path to the target.

Table 7: Comparison between shortest path calculated by the memEAPF compared with the proposed MOE-APF method in terms of path length, optimization time, path roughness, and the number of configuration points.

	The memEAPF method				**The proposed MOE-APF method**			
Environment	Path length (m)	Optimization time (s)	Path roughness	Number of configurations	Path length (m)	Optimization time (s)	Path roughness	Number of configurations
1	6.435	0.247	0.530	51	5.311	0.205	0.340	14
2	9.033	0.224	2.730	10	8.141	0.224	0.320	21
3	9.481	0.326	3.630	10	8.705	0.253	0.370	22
4	10.023	0.160	5.110	13	6.149	0.181	0.210	16
5	6.500	0.275	0.000	51	6.500	0.226	0.000	17
6	10.552	0.406	78.150	51	8.829	0.284	1.320	23
7	8.721	0.509	77.480	51	6.923	0.451	1.050	18

8	18.415	0.794	240.510	145	8.368	0.676	5.570	21
9	9.464	0.161	0.580	49	7.059	0.129	0.440	18
10	5.255	0.718	4.480	9	4.672	0.412	0.030	12
11	9.019	0.438	0.750	51	8.126	0.333	0.210	21
12	9.875	0.403	4.670	51	8.678	0.201	0.860	22

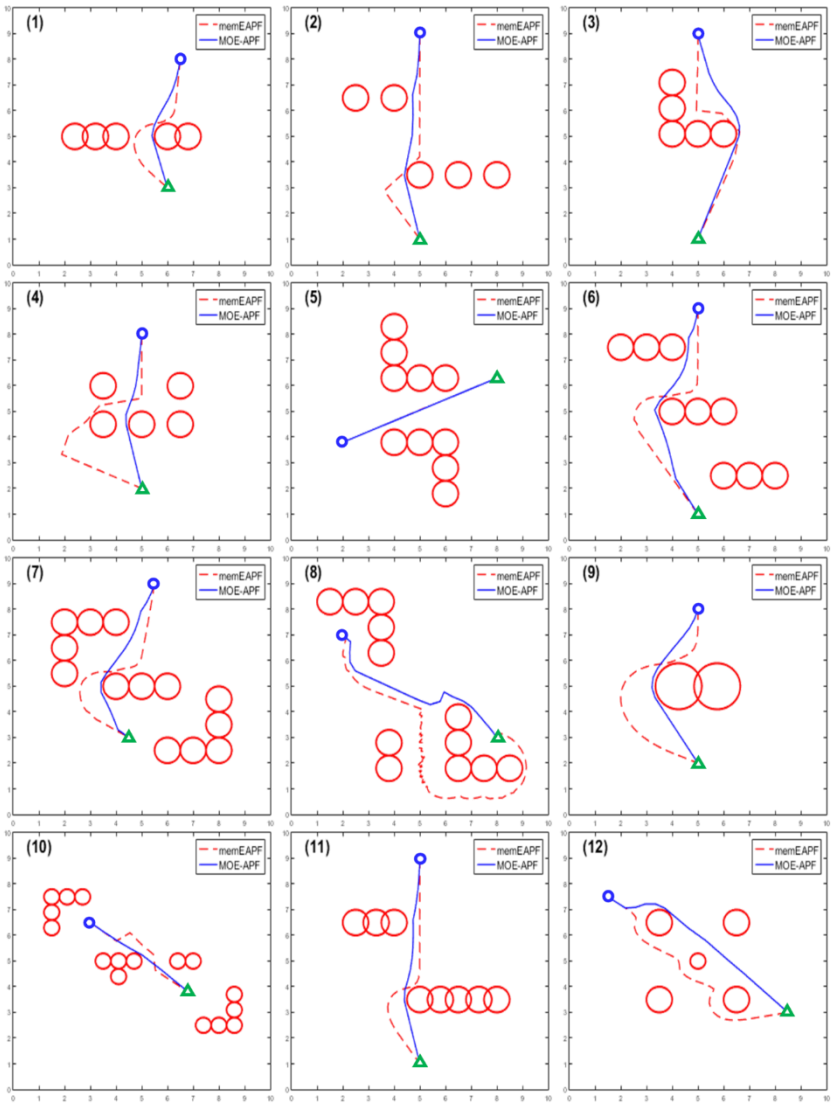

Fig 10: Comparison between shortest paths calculated by the memEAPF and the MOE-APF methods

7. Conclusion

This article presents a novel path planning method called MOE-APF that demonstrates a high performance in terms of time efficiency, path length optimization, path smoothness, and success rate. In the proposed method, the repulsive field is modified by two factors. First, the relative distance between the MR and the target position is added. Second, a rotational matrix is added so that the repulsive force makes the MR follow the obstacle contour rather than repels it away. In addition, an evolutionary algorithm is used for automatic selection of the APF parameters. The evolutionary algorithm employed a multi-objective fitness function that

incorporates path length, path roughness, and path safety. Based on statistical analysis, the step size is set to a constant value and removed from the optimization parameter set. Meanwhile, the repulsive rotational angle and the obstacle distance of influence are added to the optimization set.

A comparison is done between a previous method called memEAPF and the proposed MOE-APF. Through experimentation and analysis, the proposed method showcases its effectiveness and outperforms the memEAPF method in all performance measures, which are path length, path smoothness, path safety, success rate, and optimization time. However, the proposed method results in low quality paths in environments that require maneuver in an opposite direction. This is because the MOE-APF employs a single rotational angle along the full path. This problem can be solved by continuously searching for the best rotational angle along the path. The low optimization time of the proposed method open the door for an online version, which automatically re-optimizes the APF parameters to refine the initial calculated path.

References

[1] Rubio, F., F. Valero, and C. Llopis-Albert, *A review of mobile robots: Concepts, methods, theoretical framework, and applications.* International Journal of Advanced Robotic Systems, 2019. **16**(2).

[2] Niloy, M.A.K., et al., *Critical Design and Control Issues of Indoor Autonomous Mobile Robots: A Review.* IEEE Access, 2021. **9**: p. 35338-35370.

[3] Tsagaris, A., P. Kyratsis, and G. Mansour, *The Integration of Genetic and Ant Colony Algorithm in a Hybrid Approach.* International Journal of Intelligent Systems and Applications in Engineering, 2023. **11**(2): p. 336 – 342.

[4] Ajani, S.N., et al., *Dynamic RRT* Algorithm for Probabilistic Path Prediction in Dynamic Environment.* International Journal of Intelligent Systems and Applications in Engineering, 2023. **11**(7s): p. 263 - 271.

[5] Tan, C.S., R. Mohd-Mokhtar, and M.R. Arshad, *A Comprehensive Review of Coverage Path Planning in Robotics Using Classical and Heuristic Algorithms.* IEEE Access, 2021. **9**: p. 119310-119342.

[6] Dong, L., et al., *A review of mobile robot motion planning methods: from classical motion planning workflows to reinforcement learning-based architectures.* Journal of Systems Engineering and Electronics, 2023. **34**(2): p. 439-459.

[7] Wang, J., et al., *Neural RRT*: Learning-Based Optimal Path Planning.* IEEE Transactions on Automation Science and Engineering, 2020. **17**(4): p. 1748-1758.

[8] Sasagawa, A., S. Sakaino, and T. Tsuji, *Motion Generation Using Bilateral Control-Based Imitation Learning With Autoregressive Learning.* IEEE Access, 2021. **9**: p. 20508-20520.

[9] Ataollahi, M. and M. Farrokhi, *Online path planning of cooperative mobile robots in unknown environments using improved Q-Learning and adaptive artificial potential field.* The Journal of Engineering, 2023. **2023**(2).

[10] Arambula Cosío, F. and M.A. Padilla Castañeda, *Autonomous robot navigation using adaptive potential fields.* Mathematical and Computer Modelling, 2004. **40**(9-10): p. 1141-1156.

[11] Wahab, M.N.A., S. Nefti-Meziani, and A. Atyabi, *A comparative review on mobile robot path planning: Classical or meta-heuristic methods?* Annual Reviews in Control, 2020. **50**: p. 233-252.

[12] Cao, M., B. Li, and M. Shi, *The Dynamic Path Planning of Indoor Robot Fusing B-Spline and Improved Anytime Repairing A* Algorithm.* IEEE Access, 2023. **11**: p. 92416-92423.

[13] Zhang, W., Y. Xu, and J. Xie, *Path Planning of USV Based on Improved Hybrid Genetic Algorithm*, in *2019 European Navigation Conference (ENC)*. 2019. p. 1-7.

[14] Montiel, O., R. Sepúlveda, and U. Orozco-Rosas, *Optimal Path Planning Generation for Mobile Robots using Parallel Evolutionary Artificial Potential Field.* Journal of Intelligent & Robotic Systems, 2014. **79**(2): p. 237-257.

[15] Koren, Y. and J. Borenstein, *Potential field methods and their inherent limitations for mobile robot navigation*, in *Proceedings of the 1991 IEEE International Conference on Robotics and Automation*. 1991. p. 7.

[16] Mohamed, A., N. Ziedan, and T. Gaafar, *Artificial Potential Field Approaches for Indoor Mobile Robot Path Planning: A Review.* The Egyptian International Journal of Engineering Sciences and Technology, 2023. **0**(0): p. 0-0.

[17] Khatib, O., *Real-time obstacle avoidance for manipulators and mobile robots*, in *Proceedings. 1985 IEEE International Conference on Robotics and Automation*. 1985. p. 500-505.

[18] Ge, S.S. and Y.J. Cui, *New potential functions for mobile robot path planning.* IEEE Transactions on Robotics and Automation, 2000. **16**(5): p. 615-620.

[19] Raja, R., A. Dutta, and K.S. Venkatesh, *New potential field method for rough terrain path planning using genetic algorithm for a 6-wheel rover*. Robotics and Autonomous Systems, 2015. **72**: p. 295-306.

[20] Zhou, Z., et al., *Tangent navigated robot path planning strategy using particle swarm optimized artificial potential field*. Optik, 2018. **158**: p. 639-651.

[21] Zhang, T., J. Xu, and B. Wu, *Hybrid Path Planning Model for Multiple Robots Considering Obstacle Avoidance.* IEEE Access, 2022. **10**: p. 71914-71935.

[22] Chen, G. and J. Liu, *Mobile Robot Path Planning Using Ant Colony Algorithm and Improved Potential Field Method.* Comput Intell Neurosci, 2019. **2019**: p. 1932812.

[23] Orozco-Rosas, U., O. Montiel, and R. Sepúlveda, *Mobile robot path planning using membrane evolutionary artificial potential field.* Applied Soft Computing, 2019. **77**: p. 236-251.

[24] Sfeir, J., M. Saad, and H. Saliah-Hassane, *An improved Artificial Potential Field approach to real-time mobile robot path planning in an unknown environment*, in *2011 IEEE International Symposium on Robotic and Sensors Environments (ROSE)*. 2011. p. 208-213.

[25] Li, H., *Robotic Path Planning Strategy Based on Improved Artificial Potential Field*, in *2020 International Conference on Artificial Intelligence and Computer Engineering (ICAICE)*. 2020. p. 67-71.

[26] Goricanec, J., et al., *Collision-Free Trajectory Following With Augmented Artificial Potential Field Using UAVs.* IEEE Access, 2023. **11**: p. 83492-83506.

[27] Zhang, T., Y. Zhu, and J. Song, *Real-time motion planning for mobile robots by means of artificial potential field method in unknown environment.* Industrial Robot: An International Journal, 2010. **37**(4): p. 384-400.

[28] Jayaweera, H.M. and S. Hanoun, *A Dynamic Artificial Potential Field (D-APF) UAV Path Planning Technique for Following Ground Moving Targets.* IEEE Access, 2020. **8**: p. 192760-192776.

[29] Yao, Q., et al., *Path Planning Method With Improved Artificial Potential Field—A Reinforcement Learning Perspective.* IEEE Access, 2020. **8**: p. 135513-135523.

[30] Chen, Y., et al., *Path Planning and Obstacle Avoiding of the USV Based on Improved ACO-APF Hybrid Algorithm With Adaptive Early-Warning.* IEEE Access, 2021. **9**: p. 40728-40742.

[31] Luo, J., Z.-X. Wang, and K.-L. Pan, *Reliable Path Planning Algorithm Based on Improved Artificial Potential Field Method.* IEEE Access, 2022. **10**: p. 108276-108284.

[32] Szczepanski, R., T. Tarczewski, and K. Erwinski, *Energy Efficient Local Path Planning Algorithm Based on Predictive Artificial Potential Field.* IEEE Access, 2022. **10**: p. 39729-39742.

[33] Mitchell, M., *An Introduction to Genetic Algorithms*. 1998.

[34] Nazarahari, M., E. Khanmirza, and S. Doostie, *Multi-objective multi-robot path planning in continuous environment using an enhanced genetic algorithm.* Expert Systems with Applications, 2019. **115**: p. 106-120.